Bidirectional synaptic plasticity in the cerebellum-like mammalian dorsal cochlear nucleus

Kiyohiro Fujino* and Donata Oertel†

Department of Physiology, University of Wisconsin, 1300 University Avenue, Madison, WI 53706

The dorsal cochlear nucleus integrates acoustic with multimodal sensory inputs from widespread areas of the brain. Multimodal inputs are brought to spiny dendrites of fusiform and cartwheel cells in the molecular layer by parallel fibers through synapses that are subject to long-term potentiation and long-term depression. Acoustic cues are brought to smooth dendrites of fusiform cells in the deep layer by auditory nerve fibers through synapses that do not show plasticity. Plasticity requires Ca^{2+}-induced Ca^{2+} release; its sensitivity to antagonists of *N*-methyl-D-aspartate and metabotropic glutamate receptors differs in fusiform and cartwheel cells.

Auditory nerve fibers bring acoustic information to the cochlear nucleus and feed it into several parallel pathways that ascend through the brainstem. Pathways through the dorsal cochlear nucleus (DCN) are thought to detect spectral cues for localizing sounds monaurally (1). Those through the ventral cochlear nucleus (VCN) encode spectral and temporal characteristics that allow sounds to be localized in the horizontal plane, through binaural circuits, and recognized.

The DCN resembles the cerebellum, cartwheel cells being homologues of cerebellar Purkinje cells (2). Fusiform cells project to the inferior colliculus. Granule cells in the vicinity of the cochlear nuclei are innervated by diverse regions of the brain, including the dorsal column nuclei (1), vestibular periphery (3), and auditory nuclei (4, 5). Their unmyelinated axons, parallel fibers, contact spiny dendrites of fusiform and cartwheel cells. Myelinated auditory nerve fibers contact smooth basal dendrites of fusiform cells. The DCN resembles the electrosensory lobes in fishes even more closely (6, 7).

In cerebellar circuits, the gain of one of two converging systems of inputs varies as a function of activity. Long-term depression (LTD) at parallel fiber synapses in cerebellar Purkinje cells evoked by coincident excitation through parallel fiber and climbing fiber synapses plays a role in coordination and motor learning (8). Long-term potentiation (LTP) and LTD at parallel fiber synapses are evoked in electric fishes by convergent excitation by parallel fibers and sensory afferents to compensate for an animal's own signals in localizing external sources (9). We show that principal cells of the DCN combine multimodal inputs through parallel fibers whose strength is modulated by activity with invariant acoustic input through auditory nerve fibers.

Methods

Coronal slices (200 μm) containing the DCN were prepared from ICR mice (Harlan–Sprague–Dawley) between 18 and 20 days old with an oscillating tissue slicer (VT1000S, Leica Microsystems, Nussloch, Germany). Slices were held in a 300-μl chamber that was superfused at 3–5 ml/min with oxygenated saline at ≈33°C. Experiments were done in accordance with the protocols and guidelines of the Animal Care and Use Committee at the University of Wisconsin, Madison.

Whole-cell patch-clamp recordings were generally made with 3- to 5-MΩ pipettes filled with a K-gluconate-based solution. Voltages and currents were measured through an Axopatch 200B amplifier, low-pass filtered at 5 kHz and digitized at 16.7–25 kHz through a Digidata 1200 interface (Axon Instruments, Foster City, CA). Voltages were corrected for junction potentials, −5 to −12 mV

depending on the solutions. Series resistance was compensated to >95%. Stimulus generation, data acquisition, and analyses were performed with PCLAMP software (Axon Instruments). Cells were held at −80 mV. Shocks (5- to 100-V amplitude, 100-μs duration) were generated by a stimulator (Master-8, AMPI, Jerusalem) and delivered through a saline-filled glass pipette (3–5 μm in diameter) to the molecular or deep layer between 100 and 200 μm from the recording site. Stimulus strength was set to evoke the largest possible excitatory postsynaptic current (EPSC). EPSCs were monitored at 0.1 Hz. Cells' input resistances were monitored by −10-mV voltage steps. Potentiation and depression were quantified as the ratio of the mean amplitude of EPSCs over a 5-min period between 25 and 30 min or 55 and 60 min, referred to as 30 or 60 min after the conditioning stimulus, respectively, and the mean amplitude before the conditioning stimuli. Cells were excluded from analysis if there was >20% change of input resistance or if the mean amplitudes of EPSCs for every minute during the control period varied by >10% from the overall mean amplitude during the control period. In plots from individual cells (ordinates in pA), each point represents the mean ± SE for six consecutive responses over 1 min. Plots of normalized responses (ordinate is %EPSC) show mean ± SE of responses from different cells. Numerical data are presented as mean ± SD with number of cells tested.

In most experiments, the pipettes contained (in mM) 113 K-gluconate, 4.5 $MgCl_2$, 14 $Tris_2$-phosphocreatine, 9 Hepes, 0.1 EGTA, 4 Na_2-ATP, and 0.3 Tris-GTP (pH adjusted to 7.25 with KOH). In some experiments, 0.1% biocytin was added to the pipette. In experiments in which the intracellular calcium concentration was strongly buffered, pipettes contained (in mM) 108 K-gluconate, 4.5 $MgCl_2$, 14 $Tris_2$-phosphocreatine, 9 Hepes, 9 EGTA, 4 Na_2-ATP, and 0.3 Tris-GTP (pH 7.25). Recordings in Fig. 1 *A–C* were made with pipettes filled with a CsCl-based solution (in mM): 140 CsCl/1 KCl/1 NaCl/3 $MgCl_2$/9 Hepes/10 EGTA/2 QX-314/0.1% biocytin; pH was adjusted to 7.25 with CsOH. Ryanodine and thapsigargin (Calbiochem) were dissolved in DMSO, resulting in a 0.1% concentration of DMSO in the pipette. Ten millimolar caffeine replaced 5 mM K-gluconate in the pipette solution.

The normal external saline contained (in mM): 130 NaCl, 3 KCl, 1.2 KH_2PO_4, 2.4 $CaCl_2$, 1.3 $MgSO_4$, 20 $NaHCO_3$, 3 Hepes, and 10 glucose; saturated with 95% O_2/5% CO_2; pH adjusted to 7.4 with NaOH. To prevent precipitation, LY341495 (Tocris) was added to a Hepes-buffered saline (in mM): 138 NaCl/4.2 KCl/2.4 $CaCl_2$/1.3 $MgCl_2$/10 Hepes/10 glucose; saturated with 100% O_2; pH 7.4. Glycinergic and $GABA_A$ergic inhibitory inputs were routinely blocked by 1 μM strychnine and 50 μM picrotoxin. DNQX (6,7-dinitroquinoxaline-2,3-dione), APV (2-amino-5-phosphonovaleric acid), transACPD (t-ACPD, Tocris, Ellisville, MO), and

NEUROSCIENCE
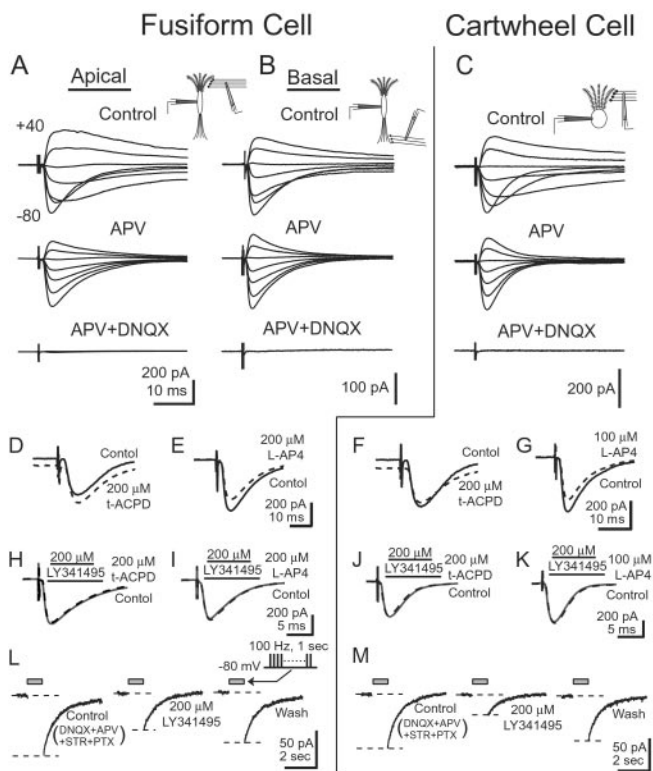
Fig. 1. Glutamatergic receptors of the AMPA, NMDA, and mGluR subtypes contribute to synaptic responses in fusiform and cartwheel cells. (*A*) In a fusiform cell, EPSCs were evoked by stimulating the molecular layer while the holding potential of the cell was varied between −80 and +40 mV in 20-mV steps. A slow component that was prominent at depolarizing holding potentials was blocked by 50 μM APV, indicating that it was mediated through NMDA receptors. The remaining fast component was blocked by 20 μM DNQX, showing that it was mediated through AMPA receptors. (*B*) In a different fusiform cell, EPSCs were evoked through the deep layer. EPSCs contained currents through both NMDA and AMPA receptors. (*C*) In a cartwheel cell, EPSCs evoked by shocks to the molecular layer had a relatively large current through NMDA receptors. (*D*) In a fusiform cell, 200 μM t-ACPD shifted the holding current at −80 mV inwardly but did not change the amplitude of the EPSC evoked by a shock to parallel fibers. (*E*) Two hundred micromolar L-AP4 decreased the amplitude of EPSCs evoked by stimulating parallel fibers but did not shift the holding current. (*F*) In a cartwheel cell, 200 μM t-ACPD shifted the holding current inwardly and decreased the amplitude of the EPSCs. (*G*) In another cartwheel cell, 100 μM L-AP4 decreased the amplitude of EPSCs without shifting the holding current. (*H–K*) Maximal responses to either t-ACPD or L-AP4 were blocked by LY341495. Solid gray line shows response to parallel fiber stimulation in the presence of 200 μM LY341495. Dashed black line shows response in the additional presence of agonist. (*L* and *M*) Train of shocks to parallel fibers, 100 Hz, 1 sec [gray bar (*Inset*), with stimulus artifacts removed], reveals a current mediated by mGluR. A slow inward current after the shocks was evoked in the presence of 20 μM DNQX and 100 μM APV at −80 mV. The inward current was partially but reversibly blocked by 200 μM LY341495.

L-AP4 (Tocris) were added to the normal saline. All drugs were obtained from Sigma unless otherwise noted.

In some experiments, cells were labeled with biocytin. Slices were fixed in 4% paraformaldehyde, embedded in a mixture of gelatin and albumin, and resectioned. Biocytin-filled cells were visualized with horseradish peroxidase (Vectastain ABC Elite Kit, Vector Laboratories).

Results

EPSCs and Their Glutamatergic Receptors in Fusiform and Cartwheel Cells.
The large cell bodies in the fusiform cell layer of the DCN belong almost exclusively to fusiform and cartwheel cells. Iden-

tification of cells was based on electrophysiological criteria developed previously (10–12). Depolarizing current evoked trains of uniform action potentials in fusiform and complex action potentials in cartwheel cells. The resting potentials were −58.6 ± 4.1 mV in fusiform cells ($n = 195$) and −64.6 ± 11.1 mV in cartwheel cells ($n = 181$).

Three excitatory synaptic responses were compared: (*i*) parallel fiber inputs to apical dendrites of fusiform cells, (*ii*) auditory nerve inputs to basal dendrites of fusiform cells, and (*iii*) parallel fiber inputs to cartwheel cells. The deep layer contains axons from two possible sources of excitation, auditory nerve fibers and T stellate cells (13). For simplicity, we will attribute all responses to stimulation in the deep layer to auditory nerve fibers because no heterogeneity was detected. EPSCs were mediated through *N*-methyl-D-aspartate (NMDA) and AMPA receptors. Fifty-micromolar APV, an antagonist of NMDA receptors, decreased the amplitude and duration of synaptic currents measured at depolarized potentials. The APV-insensitive currents were blocked by 20 μM DNQX, indicating that they are mediated through AMPA receptors (Fig. 1 *A–C*).

TransACPD (t-ACPD), an agonist for group 1 and 2 metabotropic glutamate receptors (mGluRs) (14), and L-AP4, an agonist for group 3 mGluRs (15), were used to test for the contribution of mGluRs to synaptic transmission between parallel fibers and their fusiform and cartwheel cell targets (14, 16, 17). Applications were made while the holding current and the amplitude of EPSCs evoked by stimulation of parallel fibers were monitored. Dose–response relationships for t-ACPD were sigmoid, saturating at ≈100 μM. At 200 μM, t-ACPD shifted the holding current inwardly in fusiform (70.3 ± 20.1 pA, $n = 10$; Fig. 1*D*) and cartwheel cells (67.5 ± 20.9 pA, $n = 8$; Fig. 1*F*). In cartwheel cells, t-ACPD also decreased the amplitude of the EPSCs (32.1 ± 6.1% decrease, $n = 8$; Fig. 1*F*). The actions of t-ACPD had an EC_{50}, when fit with a Hill function, near 25 μM for all these effects (fusiform holding current 28.3 μM; cartwheel holding current 26.6 μM; cartwheel EPSC 22.2 μM). L-AP4 decreased EPSCs in both fusiform and cartwheel cells. Its dose–response relationships were sigmoid, saturating at ≈100 μM. At saturating concentrations, L-AP4 decreased EPSCs in fusiform cells (200 μM, 16.5 ± 3.6% decrease, $n = 7$; Fig. 1*E*) and cartwheel cells (100 μM, 15.6 ± 6.7% decrease, $n = 6$; Fig. 1*G*) without changing the holding current. The EC_{50} of the effects of L-AP4 on EPSCs was ≈15 μM (fusiform EPSCs 17.1 μM; cartwheel EPSCs 11.6 μM). An antagonist for all subtypes of mGluRs, LY341495 (18), was tested for its ability to antagonize maximal responses to agonists. At 200 μM, LY341495 blocked all mGluR-mediated responses in fusiform (200 μM t-ACPD, $n = 4$; 200 μM L-AP4, $n = 3$; Fig. 1 *H* and *I*) and cartwheel cells (200 μM t-ACPD, $n = 4$; 100 μM L-AP4, $n = 3$; Fig. 1 *J* and *K*). If effects on the holding current are interpreted as postsynaptic actions and effects on the amplitude of the EPSC as presynaptic actions, then these results largely support conclusions from other types of studies that synapses between parallel fibers and fusiform and cartwheel cells are affected postsynaptically by group 1 and/or 2 mGluRs and presynaptically by group 3 mGluRs (14, 16, 17). Group 1 mGluRs may also have a presynaptic action at cartwheel cell synapses, although some authors have argued that all effects of group 1 mGluRs are postsynaptic (14).

To determine whether mGluRs in fusiform and cartwheel cells mediate responses to parallel fibers, the sensitivity to 200 μM LY341495 was tested of responses to trains of shocks. After the end of such a train (100 Hz, 1 sec) presented in the presence of 20 μM DNQX and 100 μM APV, an inward current was detected in fusiform and cartwheel cells. Part of this current was blocked reversibly by 200 μM LY341495, indicating that part of the current was mediated through mGluRs (fusiform 51.4 ± 8.7%, $n = 3$; cartwheel 59.7 ± 2.9%, $n = 3$; Fig. 1 *L* and *M*). The mean

peak amplitude of the LY341495-sensitive difference current was 33.7 ± 3.5 pA in fusiform cells and 41.3 ± 10.2 pA in cartwheel cells. The receptors that mediate the remaining current have not been identified.

Synaptic Plasticity at Parallel Fiber Synapses in Fusiform and Cartwheel Cells Is Bidirectional and Reversible. Long-term changes in EPSCs could be induced at synapses between parallel fibers and their targets. Pairing of trains of high-frequency shocks to the parallel fibers with depolarization of a target cell (HFS) induced LTP in both fusiform and cartwheel cells (Fig. 2 *A* and *B*). Twice with a 20-sec interval, a train of shocks was given to the molecular layer at 100 Hz for 1 sec while the postsynaptic cell was depolarized with a voltage pulse from −80 to −30 mV. The amplitude of EPSCs was then monitored at −80 mV and 0.1 Hz. In fusiform cells, HFS caused a long-lasting increase in EPSCs to 138.2 ± 7.7% at 30 min and 141.4 ± 6.6% at 60 min after HFS (*n* = 11). In cartwheel cells, HFS caused an increase to 144.7 ± 17.2% at 30 min and 136.9 ± 15.3% at 60 min after HFS (*n* = 10). LTP, defined here as an increase of at least 10% in the average amplitude of EPSCs 30 min after HFS, was observed in 16 of 18 fusiform and 15 of 17 cartwheel cells. The amplitude of EPSCs was not affected by depolarization alone in any of the five fusiform and five cartwheel cells tested. HFS without depolarization evoked LTP in two of four fusiform and two of four cartwheel cells, presumably because imperfect voltage-clamp allowed some cells to be depolarized synaptically. Pairing of low-frequency shocks at 1 Hz for 5 min with postsynaptic 60-ms voltage pulses to −30 mV (LFS) induced LTD in fusiform and cartwheel cells (Fig. 2 *C* and *D*). In fusiform cells, the EPSCs were 73.6 ± 8.6% at 30 min and 75.1 ± 10.9% at 60 min after LFS (*n* = 7). In cartwheel cells, EPSCs were 70.9 ± 9.6% at 30 min and 77.1 ± 10.5% at 60 min after LFS (*n* = 7). LTD, at least 10% decrease in the EPSC 30 min after LFS, was observed in 18 of 22 fusiform and 15 of 18 cartwheel cells. Synaptic stimulation at 1 Hz for 5 min without depolarization evoked no depression in any of the cells tested (three fusiform and three cartwheel). Depolarization without synaptic stimulation also did not evoke depression (three fusiform and three cartwheel). Potentiation and depression could be reversed in fusiform (*n* = 3) and cartwheel cells (*n* = 3) (Fig. 2 *E* and *F*). Postsynaptic fluctuation in intracellular Ca^{2+} concentration is required for potentiation and depression because LTP and LTD were not observed when recordings were made with pipette solutions that contained 9 mM EGTA (three cells each for LTP and LTD in both cell types; Table 1).

Fusiform cells receive input from parallel fibers on apical dendrites and from auditory nerve fibers on basal dendrites. To compare potentiation at the two groups of synapses, responses to shocks delivered by the same pipette first to the deep layer and then to the molecular layer were recorded from the cell bodies of fusiform cells. HFS in the deep layer produced no potentiation, but subsequent HFS in the molecular layer potentiated EPSCs in the same fusiform cell (*n* = 3; Fig. 2*G*). Similarly, LFS in the deep layer did not evoke LTD, even when subsequent LFS in the molecular layer did (*n* = 3; Fig. 2*H*). Neither LTP (*n* = 12) nor LTD (*n* = 9) was observed in responses to stimulation in the deep layer. LFS at 0.1 Hz paired with depolarization did not evoke LTD either at auditory nerve synapse (*n* = 3).

Sensitivity of LTP and LTD to Blockers of NMDA and mGluRs. The sensitivity of LTP to blockers of NMDA and mGluRs differed in fusiform and cartwheel cells (Table 1). In some fusiform cells, blocking NMDA receptors with 100 μM APV blocked LTP, but in others it did not (Fig. 3 *A* and *B*). Similar tests showed that blocking mGluRs with 200 μM LY341495 blocked LTP in only some fusiform cells (Fig. 3 *D* and *E*). LTP was also observed in the presence of the combination of APV and LY341495, indi-
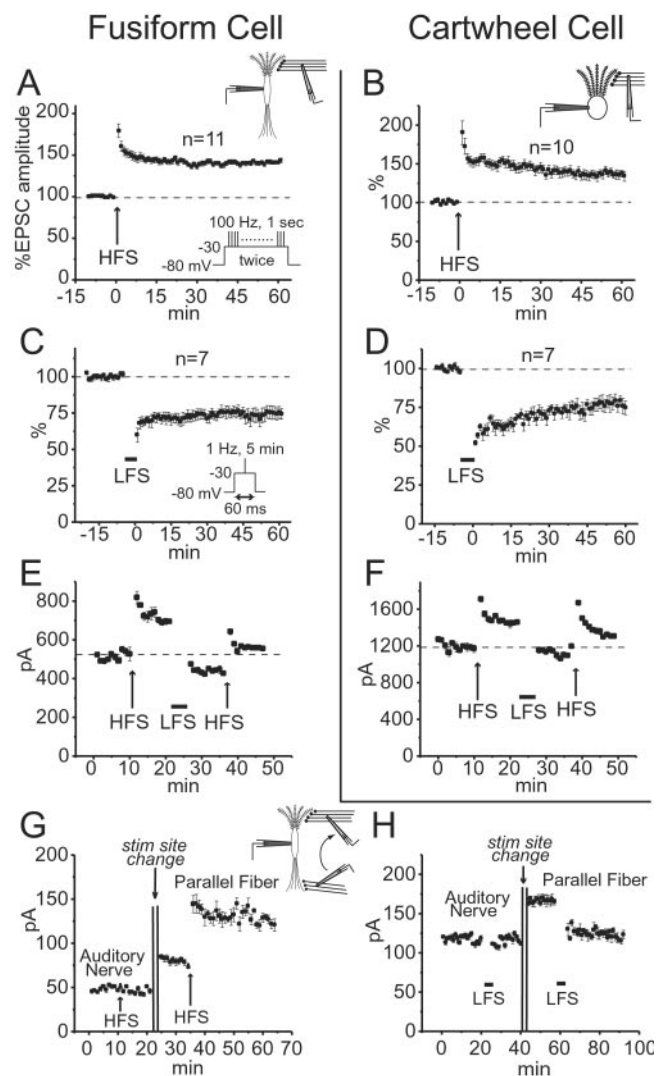

Fig. 2. Bidirectional plasticity was observed in responses to shocks of parallel fibers in fusiform and cartwheel cells but not in responses to shocks of auditory nerve fibers. (*A* and *B*) LTP was evoked in fusiform and cartwheel cells by HFS. HFS comprised two repetitions with a 20-sec interval of depolarizing the postsynaptic cell from −80 to −30 mV for 1 sec while stimulating parallel fibers for 100 Hz (*A Inset*). Plots show mean, normalized EPSC amplitudes from all cells in which recordings were made for >60 min after HFS. (*C* and *D*) LTD was evoked in fusiform and cartwheel cells by LFS. LFS comprised stimulating parallel fibers at 1 Hz for 5 min, each shock being presented during a 60-ms depolarization of the postsynaptic cell from −80 to −30 mV (*C Inset*). Plots show mean normalized EPSC amplitudes from all cells in which recordings were made for >60 min after LFS. (*E* and *F*) In a fusiform and a cartwheel cell, potentiation and depression could be reversed. (*G*) In a fusiform cell, LTP could not be induced by stimulation in the deep layer, but could subsequently be induced by moving the stimulating electrode to the molecular layer. (*H*) In a fusiform cell, LTD could not be induced with stimulation in the deep layer, but could subsequently be induced by moving the stimulating pipette to the molecular layer.

cating that other receptors contribute to the induction of LTP (Fig. 3*H*). To test whether the strength of potentiation might have been reduced in those fusiform cells in which LTP was not blocked by APV and LY341495, responses were normalized and averaged over all cells in which LTP was observed. Both APV and LY341495 individually and in combination decreased the mean amplitude of LTP (Fig. 3*J*). Averaged amplitudes of EPSCs 30 min after HFS were significantly different from one another under all conditions (*P* < 0.01, unpaired *t* test). The

NEUROSCIENCE

Table 1. Summary of the pharmacological properties of LTP and LTD in the DCN

	APV		LY341495		APV + LY341495		High EGTA		Ryanodine		Caffeine + thapsigargin	
	Absent	Present	Absent	Present	Absent	Present	Absent	Present	Absent	Present	Absent	Present
Fusiform LTP	9	9	5	3	5	1	3	0	8	1	5	0
Cartwheel LTP	0	5	0	10	0	3	3	0	5	3	6	0
Fusiform LTD	4	2	0	6	4	2	3	0	4	1	4	0
Cartwheel LTD	8	0	0	4	—	—	3	0	4	2	4	0

Numbers of cells in which the LTP and LTD were absent or present when 100 μM APV, 200 μM LY341495, or 100 μM APV and 200 μM LY341495 were applied extracellularly, and when 9 mM EGTA, 200 μM ryanodine, or 10 mM caffeine and 1 μM thapsigargin were applied intracellularly.
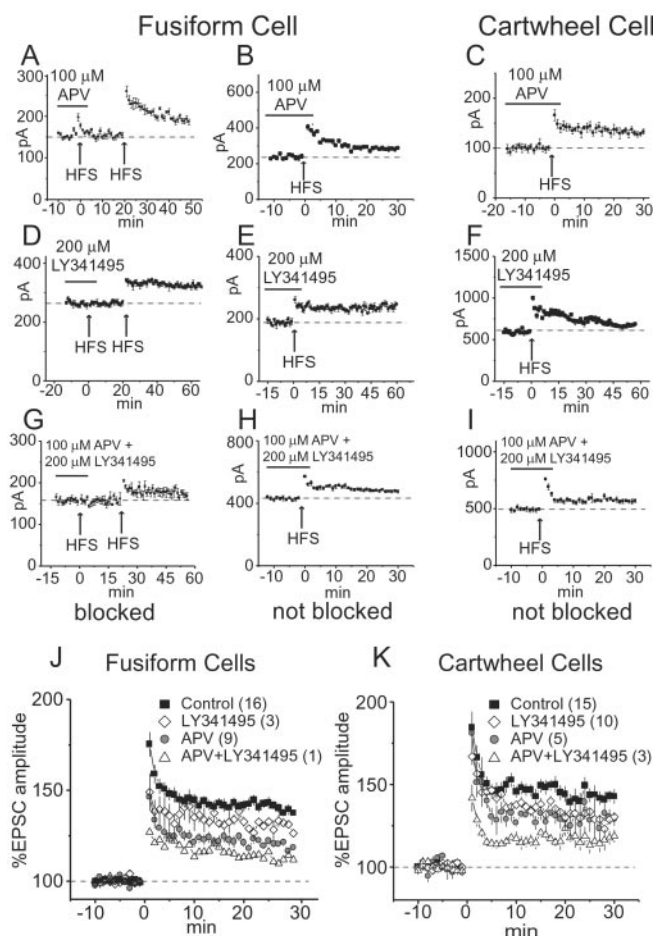
Fig. 3. NMDA and mGluRs contribute to the induction of LTP in fusiform and cartwheel cells. (A) In a fusiform cell, LTP was blocked by 100 μM APV but could subsequently be induced after APV was washed out of the bath. (B) In another fusiform cell, APV did not block the induction of LTP. (C) In a cartwheel cell, LTP was not blocked by APV. (D) In a fusiform cell, 200 μM LY341495 reversibly blocked LTP. (E) In another fusiform cell, LY341495 did not block LTP. (F) In a cartwheel cell, LY341495 failed to block LTP. (G and H) Simultaneous application of APV and LY341495 blocked LTP in one but not another fusiform cell. (I) The combination of APV and LY341495 did not block LTP in any cartwheel cell. (J and K) Plots show the mean normalized amplitudes of EPSCs for the control and the presence of LY341495 and/or APV during the conditioning stimuli. The number of cells whose responses were averaged is given in parentheses.

reduction in the average strength of LTP by each of these blockers suggests that NMDA and mGluRs each make a partial contribution.

In cartwheel cells, LTP was not blocked by 100 μM APV and 200 μM LY341495 (Fig. 3 C, F, and I). All cartwheel cells tested with HFS in the presence of APV and LY341495, alone and in combination, showed LTP (Table 1). A statistical comparison of LTP in various pharmacological conditions shows that the average magnitude of LTP was reduced by APV and LY341495 ($P < 0.01$; Fig. 3K). There was not a significant difference between application of either LY341495 or APV.

The sensitivity of LTD to antagonists of NMDA and mGluRs also differed in fusiform and cartwheel cells. In some fusiform cells, LTD could be blocked by 100 μM APV or by the simultaneous application of APV and 200 μM LY341495, but it was not blocked by LY341495 alone in any of the fusiform cells tested (Table 1, Fig. 4 A, B, D, F, and G). To test whether LTD may have been reduced even when it was not blocked, normalized, average magnitudes of EPSCs were compared in experiments where LTD was not blocked by APV or LY341495 (Fig. 4H). The differences in EPSCs averaged 30 min after LFS were significant for all four groups of experiments except between "APV" and "APV+LY341495" ($P < 0.05$). LY341495 affected the strength of LTD, although it did not block LTD in any fusiform cell. In cartwheel cells, 100 μM APV consistently blocked LTD (Table 1, Fig. 4C). Although LY341495 did not block LTD in any of the cartwheel cells tested, it significantly ($P < 0.01$) reduced its strength (Fig. 4 E and I).

Ca^{2+} Release from Internal Stores Is Required for LTP and LTD. To test whether ryanodine receptors are involved in LTP and LTD, 200 μM ryanodine in 0.1% DMSO was added to the pipette solution. In the presence of ryanodine, LTP and LTD were blocked in most of the cells tested (eight of nine in fusiform LTP, four of five in fusiform LTD, five of eight in cartwheel LTP, and four of six in cartwheel LTD; Table 1). Control experiments using pipette solutions that included 0.1% DMSO without ryanodine evoked normal plasticity in all cells tested (three of three each in fusiform LTP and LTD, and three of three each in cartwheel LTP and LTD). The interpretation of these results is complicated by ryanodine's action both as an antagonist (at high concentration) and a partial agonist (at low concentration) of ryanodine receptors (19). Plasticity may have been left unblocked because the concentration of ryanodine in distal dendrites was not high enough.

An alternative test for the involvement of Ca^{2+}-induced Ca^{2+} release through ryanodine receptors is by the intracellular application of caffeine and thapsigargin through the patch pipette. Caffeine opens ryanodine receptors, allowing Ca^{2+} to be released from the endoplasmic reticulum (20). Thapsigargin
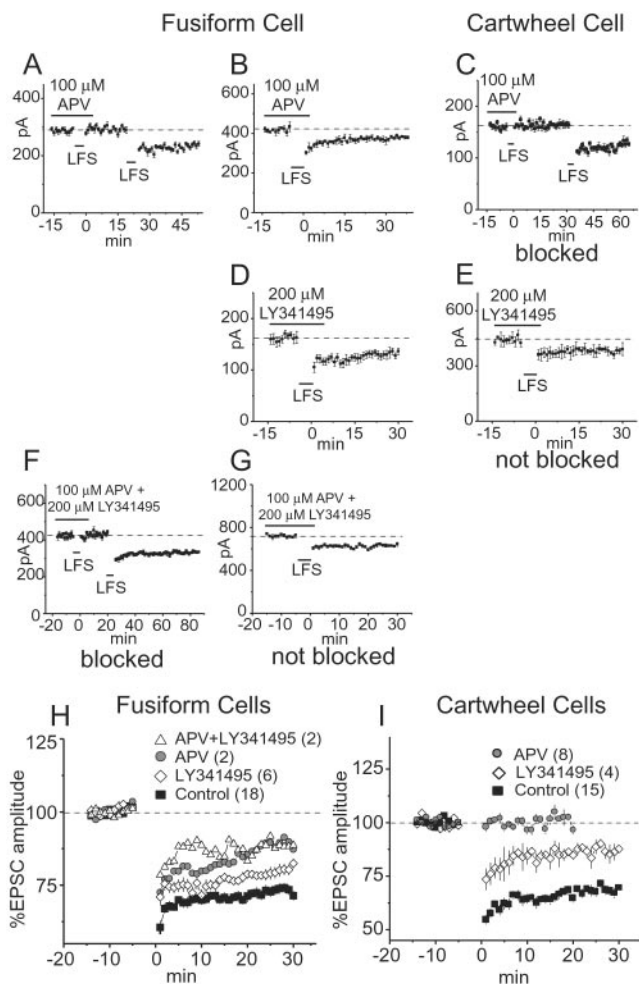
Fig. 4. NMDA and mGluRs contribute to the induction of LTD in fusiform and cartwheel cells. (*A*) In a fusiform cell, the induction of LTD by LFS was blocked by 100 μM APV but could be evoked after APV was washed out of the bath. (*B*) In another fusiform cell, LTD was not blocked by APV. (*C*) In all cartwheel cells tested, LTD was reversibly blocked by APV. (*D*) In all fusiform cells tested, 200 μM LY341495 failed to block LTD. (*E*) In all cartwheel cells, LY341495 failed to block LTD. (*F* and *G*) The simultaneous application of APV and LY341495 blocked LTD in some fusiform cells. (*H* and *I*) Averaged normalized EPSCs were compared in populations of cells. Each plot shows the mean normalized amplitudes of EPSCs in control conditions and in the presence of LY341495 and/or APV. The number of cells whose responses were averaged is given in parentheses.

blocks the ATP-dependent Ca^{2+} transport into the endoplasmic reticulum (21). HFS and LFS were applied to cells that were recorded with pipettes that contained 10 mM caffeine and 1 μM thapsigargin. Recordings were made for 30 min before HFS or LFS to allow drugs to diffuse into dendrites. No LTP or LTD was detected in any of the cells tested (Fig. 5, Table 1). These findings could not be explained by the run-down of cellular constituents because in control experiments with normal pipette solutions conditioning stimuli presented >30 min after breaking into cells did evoke plastic responses (fusiform LTP, $n = 4$; fusiform LTD, $n = 3$; cartwheel LTP, $n = 4$; and cartwheel LTD, $n = 4$; Fig. 2 *G* and *H*). The finding that plasticity could be blocked by a postsynaptic experimental manipulation shows that plasticity is initiated postsynaptically.

Discussion

In the DCN, the strength of synapses between parallel fibers and spiny fusiform and cartwheel cell dendrites, but not that of
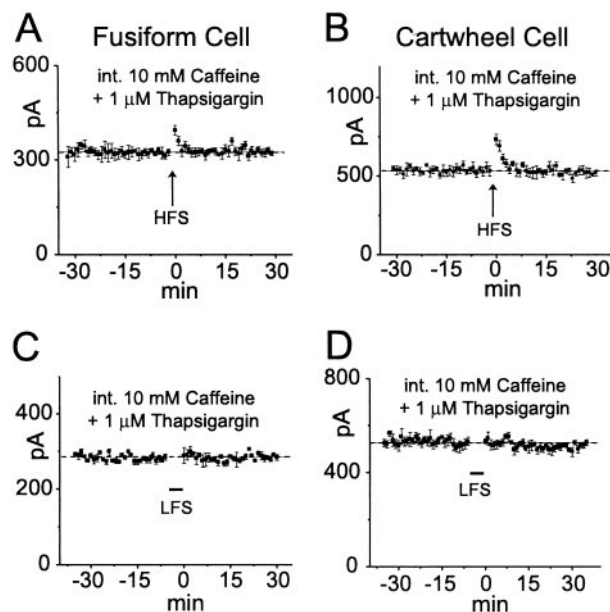
Fig. 5. Synaptic plasticity in fusiform and cartwheel cells involves Ca^{2+}-induced Ca^{2+} release. The recording pipettes contained 10 mM caffeine to release Ca^{2+} from intracellular stores and 1 μM thapsigargin to block its re-uptake. Conditioning stimuli were given after a prolonged control period (30 min) to allow the drugs to diffuse into distal dendrites.

synapses between auditory nerve fibers and smooth fusiform cell dendrites, is modulated upward and downward by activity. LTP and LTD in both fusiform and cartwheel cells is initiated postsynaptically because it can be prevented by the postsynaptic application of caffeine and thapsigargin and by the postsynaptic buffering of intracellular Ca^{2+}. The postsynaptic intracellular Ca^{2+} concentration plays a critical role in the regulation of the strength of synapses of fusiform and cartwheel cells in the molecular layer because, in the presence of strong buffering, no plasticity was observed. LTP and LTD are triggered by the activation of combinations of receptors including, but not being limited to, NMDA and mGluR. Blocking NMDA or mGluRs separately or together reduced LTP and LTD. The sensitivity of LTP and LTD to blockers of these receptors varied, indicating that their relative contributions varied among individual cells and between cell types. $GABA_B$ receptors (22) that were not blocked in this study may also modulate the induction of LTP and LTD. In cartwheel cells, but not in fusiform cells, LTD required NMDA receptors. LTP and LTD in fusiform cells were reduced by antagonists of NMDA receptors and mGluRs separately or in combination but were not consistently blocked. Ca^{2+}-induced Ca^{2+} release from intracellular stores was required for LTP and LTD in both fusiform and cartwheel cells.

The association in the DCN of synaptic plasticity with Ca^{2+} in dendritic spines parallels findings in other parts of the brain. Multiple sources of Ca^{2+} that are activated over different time courses are differentially distributed in spines and dendritic shafts. These include voltage-gated Ca^{2+} channels, Ca^{2+}-permeable ligand-gated channels, and release from intracellular stores that can be modulated by mGluRs. In the present experiments that were performed under voltage-clamp, the contribution of voltage-gated Ca^{2+} currents was presumably small; but under physiological conditions, voltage-gated Ca^{2+} currents are prominent in cartwheel cells, where they underlie the complex action potential (23, 24), and have been demonstrated in fusiform cells (25). AMPA receptors differ at the three groups of synapses in fusiform and cartwheel cells but all contain GluR2 and are thus not permeable to Ca^{2+} (16, 26, 27). NMDA

receptors are Ca^{2+}-permeable and contribute to excitation of fusiform and cartwheel cells by parallel fibers (14, 28, 29). Trains of shocks to parallel fibers evoked a slow inward current of which ≈50% was sensitive to blocking mGluRs with LY341495. If mGluR-mediated currents can be activated with shocks to parallel fibers, the mGluRs must be at or near the terminals of parallel fibers. Group 1 mGluR1α is found at synapses between parallel fibers and cartwheel cells (16, 17), but only on the basal dendrites of fusiform cells (26). mGluR5, the other group 1 mGluR, may be present in the molecular layer of the DCN (16). Group 1 mGluRs have been shown to activate phospholipase C and increase the level of IP_3, which in turn allows Ca^{2+} to be released from intracellular stores through IP_3 receptors. Cartwheel, but not fusiform, cells are labeled by antibodies to IP_3 receptors (30). The presence of vesicles in spines of cartwheel cells indicates that Ca^{2+} released from intracellular stores could act within individual spines (30, 31). Group 3 mGluRs, activated by L-AP4, act presynaptically in the DCN (14). Ca^{2+}-induced Ca^{2+} release through ryanodine receptors is required for the induction of LTP and LTD in both fusiform and cartwheel cells.

Cartwheel cells share many features of cerebellar Purkinje cells. Like Purkinje cells, cartwheel cells fire complex action potentials (10, 12), contain mGluR1α in their spines (16, 17), IP_3 in their dendrites (30), and PEP19 (32), cerebellin (33), and glutamic acid decarboxylase (34). Genetic mutations affect Purkinje cells and cartwheel cells similarly (35). Unlike Purkinje cells, cartwheel cells receive no climbing fiber input, terminate locally, and are glycinergic (23). Cartwheel cells have NMDA receptors, whereas Purkinje cells do not (36). The DCN closely resembles electrosensory lobes of fishes where principal cells and Purkinje-cell homologues receive parallel fiber input and have NMDA receptors (7, 37, 38).

A common feature of Purkinje cells and their homologues is that the strength of parallel fiber synapses is modulated by activity. In Purkinje cells, the pairing of parallel fiber input with Ca^{2+} action potentials that are driven by climbing fibers produces LTD (8). LTP has generally not been observed at synapses between parallel fibers and Purkinje cells. Purkinje cells require the synergistic action of mGluRs and a rise in IP_3 to release Ca^{2+} from intracellular stores with voltage-sensitive Ca^{2+} channels for the induction of LTD (39–41). In the absence of mGluR1 or of IP_3 receptors, LTD is not observed in Purkinje cells and motor coordination is abnormal (42–44). Blocking mGluRs, presumably a major source of IP_3, does not block LTD in cartwheel cells. In the electric fish, pairing of the stimulation of parallel fibers with postsynaptic depolarization or with broad action potentials produces both LTP and LTD in homologues of cartwheel and fusiform cells (9, 37).

There exists considerable evidence that fusiform cells, the principal cells of the DCN, are involved in the localization of sound. Fusiform cells sense the spectral distortions that are introduced by the external ear and that animals use to localize sounds in the vertical plane and monaurally (45, 46). Responses to sound are generated by the convergence of excitation through auditory nerve fibers and inhibition through inhibitory interneurons (11). Fusiform cells also sense the position of the head, neck, and pinnae through vestibular and somatosensory input to parallel fibers (1). The present work shows that fusiform cells integrate stable acoustic input through auditory nerve fibers with multimodal sensory input through parallel fibers that is modulated by activity through two pathways: direct, excitatory input from parallel fibers to fusiform cells; and indirect inhibitory input from parallel fibers through cartwheel cells (23). The convergence of acoustic and multimodal proprioceptive inputs could help mammals place spectral cues in the context of the position of head and ears for localizing sounds (1).

1. Kanold, P. O. & Young, E. D. (2001) *J. Neurosci.* **21,** 7848–7858.
2. Mugnaini, E., Warr, W. B. & Osen, K. K. (1980) *J. Comp. Neurol.* **191,** 581–606.
3. Kevetter, G. A. & Perachio, A. A. (1989) *Brain Behav. Evol.* **34,** 193–200.
4. Feliciano, M., Saldana, E. & Mugnaini, E. (1995) *Aud. Neurosci.* **1,** 287–308.
5. Golding, N. L., Robertson, D. & Oertel, D. (1995) *J. Neurosci.* **15,** 3138–3153.
6. Montgomery, J. C., Coombs, S., Conley, R. A. & Bodznick, D. (1995) *Aud. Neurosci.* **1,** 207–231.
7. Bell, C. (2002) *Brain Behav. Evol.* **59,** 312–326.
8. Ito, M. (2001) *Physiol. Rev.* **81,** 1143–1195.
9. Bell, C. C., Han, V. Z., Sugawara, Y. & Grant, K. (1997) *Nature* **387,** 278–281.
10. Zhang, S. & Oertel, D. (1993) *J. Neurophysiol.* **69,** 1384–1397.
11. Zhang, S. & Oertel, D. (1994) *J. Neurophysiol.* **71,** 914–930.
12. Manis, P. B., Spirou, G. A., Wright, D. D., Paydar, S. & Ryugo, D. K. (1994) *J. Comp. Neurol.* **348,** 261–276.
13. Oertel, D., Wu, S. H., Garb, M. W. & Dizack, C. (1990) *J. Comp. Neurol.* **295,** 136–154.
14. Molitor, S. C. & Manis, P. B. (1997) *J. Neurophysiol.* **77,** 1889–1905.
15. Bortolotto, Z. A., Fitzjohn, S. M. & Collingridge, G. L. (1999) *Curr. Opin. Neurobiol.* **9,** 299–304.
16. Petralia, R. S., Wang, Y. X., Zhao, H. M. & Wenthold, R. J. (1996) *J. Comp. Neurol.* **372,** 356–383.
17. Wright, D. D., Blackstone, C. D., Huganir, R. L. & Ryugo, D. K. (1996) *J. Comp. Neurol.* **364,** 729–745.
18. Kingston, A. E., Ornstein, P. L., Wright, R. A., Johnson, B. G., Mayne, N. G., Burnett, J. P., Belagaje, R., Wu, S. & Schoepp, D. D. (1998) *Neuropharmacology* **37,** 1–12.
19. Coronado, R., Morrissette, J., Sukhareva, M. & Vaughan, D. M. (1994) *Am. J. Physiol.* **266,** C1485–C1504.
20. Alonso, M. T., Barrero, M. J., Michelena, P., Carnicero, E., Cuchillo, I., Garcia, A. G., Garcia-Sancho, J., Montero, M. & Alvarez J. (1999) *J. Cell Biol.* **144,** 241–254.
21. Thastrup, O., Cullen, P. J., Drobak, B. K., Hanley, M. R. & Dawson, A. P. (1990) *Proc. Natl. Acad. Sci. USA* **87,** 2466–2470.
22. Juiz, J. M., Albin, R. L., Helfert, R. H. & Altschuler, R. A. (1994) *Brain Res.* **639,** 193–201.
23. Golding, N. L. & Oertel, D. (1997) *J. Neurophysiol.* **78,** 248–260.
24. Molitor, S. C. & Manis, P. B. (1999) *J. Neurophysiol.* **81,** 985–998.
25. Hirsch, J. A. & Oertel, D. (1988) *J. Physiol. (London)* **396,** 535–548.
26. Rubio, M. E. & Wenthold, R. J. (1997) *Neuron* **18,** 939–950.
27. Gardner, S. M., Trussell, L. O. & Oertel, D. (2001) *J. Neurosci.* **21,** 7428–7437.
28. Golding, N. L. & Oertel, D. (1996) *J. Neurosci.* **16,** 2208–2219.
29. Manis, P. B. & Molitor, S. C. (1996) *J. Neurophysiol.* **76,** 1639–1656.
30. Ryugo, D. K., Pongstaporn, T., Wright, D. D. & Sharp, A. H. (1995) *J. Comp. Neurol.* **358,** 102–118.
31. Wouterlood, F. G. & Mugnaini, E. (1984) *J. Comp. Neurol.* **227,** 136–157.
32. Berrebi, A. S. & Mugnaini, E. (1991) *Anat. Embryol. (Berlin)* **183,** 427–454.
33. Mugnaini, E. & Morgan, J. I. (1987) *Proc. Natl. Acad. Sci. USA* **84,** 8692–8696.
34. Mugnaini, E. (1985) *J. Comp. Neurol.* **235,** 61–81.
35. Berrebi, A. S., Morgan, J. I. & Mugnaini, E. (1990) *J. Neurocytol.* **19,** 643–654.
36. Llano, I., Marty, A., Armstrong, C. M. & Konnerth, A. (1991) *J. Physiol. (London)* **434,** 183–213.
37. Bell, C. C., Caputi, A. & Grant, K. (1997) *J. Neurosci.* **17,** 6409–6423.
38. Han, V. Z., Grant, K. & Bell, C. C. (2000) *Neuron* **27,** 611–622.
39. Linden, D. J. & Connor, J. A. (1991) *Science* **254,** 1656–1659.
40. Shigemoto, R., Abe, T., Nomura, S., Nakanishi, S. & Hirano, T. (1994) *Neuron* **12,** 1245–1255.
41. Nakamura, T., Barbara, J. G., Nakamura, K. & Ross, W. N. (1999) *Neuron* **24,** 727–737.
42. Conquet, F., Bashir, Z. I., Davies, C. H., Daniel, H., Ferraguti, F., Bordi, F., Franz-Bacon, K., Reggiani, A., Matyarese, V., Conde, F., *et al.* (1994) *Nature* **372,** 237–243.
43. Kasono, K. & Hirano, T. (1995) *NeuroReport* **6,** 569–572.
44. Miyata, M., Finch, E. A., Khiroug, L., Hashimoto, K., Hayasaka, S., Oda, S. I., Inouye, M., Takagishi, Y., Augustine, G. J. & Kano, M. (2000) *Neuron* **28,** 233–244.
45. Nelken, I. & Young, E. D. (1997) *J. Neurophysiol.* **78,** 790–799.
46. Nelken, I., Kim, P. J. & Young, E. D. (1997) *J. Neurophysiol.* **78,** 800–811.